Publications of the Korean Astronomical Society
**32**: 313 ∼ 315, 2017 March

pISSN 1225-1534
eISSN 2287-6936
https://doi.org/10.5303/PKAS.2017.32.1.313

# COMPARISON OF PHYSICAL PROPERTIES AND EVOLUTION OF AKARI AND SPITZER 24 $\mu$m-DETECTED GALAXIES AT z = 0.4 - 2

Naofumi Fujishiro[1], Hitoshi Hanami[2], and Tsuyoshi Ishigaki[2]

[1]Koyama Astronomical Observatory, Kyoto Sangyo University, Motoyama, Kamigamo, Kita-ku, Kyoto 603-8047, Japan
[2]Physics Section, Iwate University, 3-18-34 Ueda, Morioka, Iwate 020-8550, Japan

*E-mail: naofuji@cc.kyoto-su.ac.jp*

*(Received July 20, 2015; Revised October 20, 2016; Accepted October 20, 2016)*

## ABSTRACT

We present physical properties of 24 $\mu$m galaxies detected by AKARI and Spitzer and their evolution between redshifts $0.4 < z < 2$. Using multi-wavelength data from X-ray to radio observations in NEP Deep Field (for AKARI) and Subaru/XMM-Newton Deep Field (for Spitzer), we derive photometric redshift, stellar mass, star-formation rate (SFR), dust extinction magnitude and rest-frame luminosities/colors of the 24 $\mu$m galaxies from photometric SED fitting. We infer the SFRs from rest-frame ultraviolet luminosity and total infrared luminosity calibrated against Herschel photometric data. For both survey fields, we obtain complete samples with stellar mass of $> 10^{10} M_{\odot}$ and SFR of $> 30 M_{\odot}$/yr up to $z = 2$. We find that specific SFRs evolves with redshift at all stellar masses in NON-power-law galaxies (non-PLGs) as star-formation dominant luminous infrared galaxies (LIRGs). The correlations between specific SFR and stellar mass in the Spitzer and AKARI galaxy samples are well consistent with trends of the main sequence galaxies. We also discuss nature of PLGs and their evolution.

*Key words:* galaxies: evolution — galaxies: high-redshift — galaxies: active — infrared:galaxies

## 1. INTRODUCTION

The cosmic star-formation history is a major issue in observational cosmology (e.g. Madau & Dickinson, 2014). Star-formation rate density (SFRD) peaked at $z \sim 1.9$. At later times after the peak, SFRD declined exponentially with an e-folding timescale of $\sim$ 3.9Gyr. About 25% of the stellar mass observed today was formed before the peak. About 50% (75% ) formed before $z \sim 1.3$ ($z \sim 0.7$). The comoving rates of star-formation and black hole accretion follow a similar rise and fall. This similarity suggests that activities of Active Galactic Nuclei (AGN) may be closely linked to the star-formation process and its evolution. However, its internal mechanisms are still not clear.

At $0 < z < 2$, main sequence galaxies (e.g. Daddi et al., 2007) contribute to the most part of SFRD. The contribution of starburst galaxies is only ∼10%. Before JWST, the MIPS instrument on the Spitzer Space Telescope reached the deepest mid-infrared (MIR) sensitivities, while the IRC instrument of AKARI can diagnose AGN and star-formation activities in the main sequence with its continuous MIR bands (e.g. Hanami et al., 2012). However, there is very little research to study the consistency in physical properties of galaxies and AGN derived by AKARI and Spitzer.

In this paper, we focus on 24 $\mu$m-detected galaxies with AKARI/IRC and Spitzer/MIPS, and investigate the consistency in especially star-formation and AGN activities between them. We adopt a Salpeter initial mass function and a standard cosmology of WMAP.

## 2. SAMPLE SELECTION AND DATA ANAYSIS

We used multi-wavelength catalogs from X-ray to radio observations in the NEP Deep Field for AKARI (e.g. Hanami et al., 2012) and the Subaru XMM-Newton Deep Field for Spitzer (e.g. Furusawa et al., 2008). We

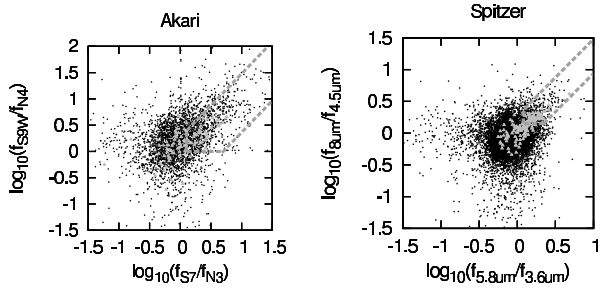


Figure 1. Power-law galaxies (PLGs) criteria (grey dotted lines) based on Donley et al. (2012). Light-grey triangles represent X-ray detected samples. Left: For AKARI objects. Right: For Spitzer objects.

selected 24 $\mu$m-detected objects with limiting AB magnitudes of $N2 < 21.9$, [24 $\mu$m]$< 18.6$ for AKARI and $K < 23.8$, [24 $\mu$m]$< 20.0$ for Spitzer. We also classified power-law galaxies (PLGs) as AGN candidates using near-IR two-color diagrams based on Donley et al. (2012) as shown in Fig.1.

For all the objects without spectroscopic redshift, we adopted photometric redshifts derived by Hyperz (e.g. Bolzonella et al., 2000) for AKARI and EAZY (e.g. Brammer et al., 2008) for Spitzer. We estimated stellar mass, $M_*$, in galaxies with population synthesis models of Bruzual & Charlot (2003) by a standard SED fitting procedure. According to Kennicutt (1998), SFRs are derived not only from intrinsic ultraviolet (UV) luminosities by assuming an extinction law, but also from IR luminosities. In order to estimate the IR luminosity, we adopt a SED fitting procedure of Hanami et al. (2012) with Siebenmorgen & Krügel (2007) models and Herschel/SPIRE data for AKARI, and an empirical law calibrated against Herschel/PACS and SPIRE data (Rujopakarn et al. (2013)) using 24 $\mu$m flux density for Spitzer. Finally, we obtained complete samples with $M_* > 10^{10} M_\odot$ and $SFR > 30 M_\odot$/yr up to $z = 2$.

## 3. PHYSICAL PROPERTIES AND EVOLUTION

Fig.2 shows stellar mass dependencies of specific SFR in non-PLGs. We have found that specific SFRs evolve with redshift at all stellar masses. The correlations between specific SFR and stellar mass in the Spitzer and AKARI samples are well consistent with evolutionary trends of the main sequence galaxies.

Fig.3 shows stellar mass dependencies of rest-frame 5 $\mu$m luminosity in 24 mm-detected PLGs with spectroscopic redshifts. The luminosities of PLGs are crearly larger than those of non-PLGs, and PLGs are easily detected by X-ray. Thus, PLGs can be selected mainly as

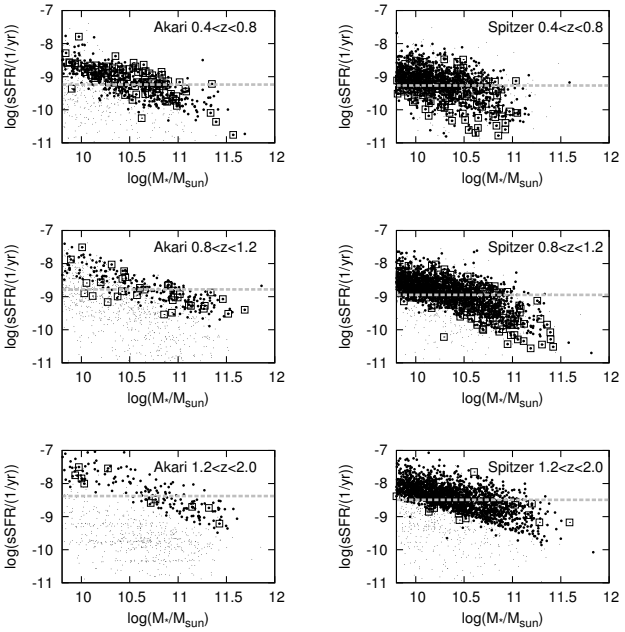


Figure 2. Stellar mass $M_*$ vs. specific $SFR$. Large dots represent 24 $\mu$m-detected objects. Small dots represent 24 $\mu$m-faint objects. Open rectangles represent samples with spectrscopic redshift. Dotted lines represent fitting results for 24 $\mu$m-detected objects. Left: For AKARI non-PLGs. Right: For Spitzer non-PLGs.

luminous MIR AGNs. If PLGs as luminous AGNs are nearly at the end of Black hole growth phase, the evolutionary trend of PLGs can be interpreted as the AGN down-sizing.

## ACKNOWLEDGMENTS

N. Fujishiro acknowledge the support from Kyoto Sangyo University and Japan Aerospace Exploration Agency (JAXA).

## REFERENCES

Bolzonella, M., Miralles, J. -M., Pello, R., 2000, Photometric Redshifts based on standard SED fitting procedures, A&A, 363, 476

Brammer, G. B., van Dokkum, P. G., Coppi, P., 2008, EAZY: A Fast, Public Photometric Redshift Code, ApJ, 686, 1503

Bruzual, G. & Charlot, S., 2003, Stellar population synthesis at the resolution of 2003, MNRAS, 344, 1000

Daddi, E., Dickinson, M., Elbaz, D., 2007, Multiwavelength Study of Massive Galaxies at z∼2. I. Star Formation and Galaxy Growth, ApJ, 670, 156

Donley, J. L., Koekemoer, A. M., Brusa, M., et al., 2012, Identifying Luminous Active Galactic Nuclei in Deep Surveys: Revised IRAC Selection Criteria, ApJ, 748, 142

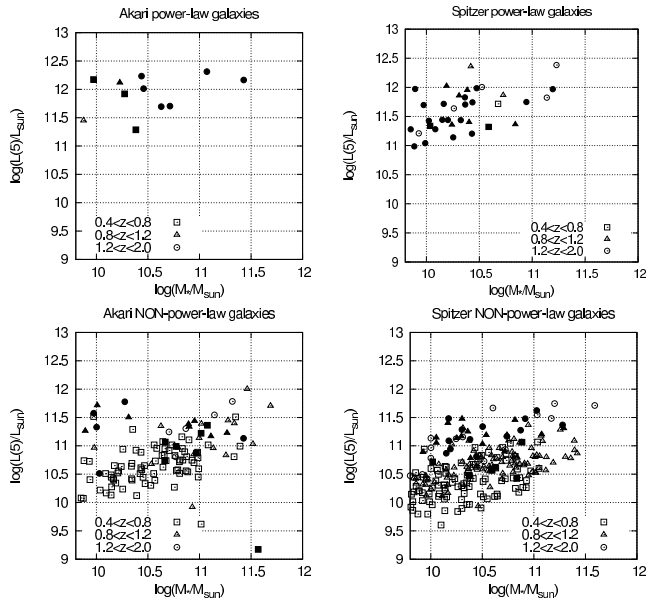


Figure 3. Stellar mass $M_*$ vs. rest-frame 5 $\mu$m luminosity for samples with spectroscopic redshift. Filled symbols represent X-ray detected samples. Top-left: For AKARI PLGs. Top-right: For Spitzer PLGs. Bottom-left: For Akari non-PLGs. Bottom-right: For Spitzer non-PLGs.

Furusawa, H., Kosugi, G., Akiyama, M., et al., 2008, The Subaru/XMM-Newton Deep Survey (SXDS). II. Optical Imaging and Photometric Catalogs, ApJS, 176, 1

Hanami, H., Ishigaki, T., Fujishiro, N., et al., 2012, Star Formation and AGN Activity in Galaxies Classified Using the 1.6$\mu$m Bump and PAH Features at z = 0.4−2, PASJ, 64, 70

Kennicutt, R. C., 1998, Star Formation in Galaxies Along the Hubble Sequence, ARA&A, 36, 189

Madau, P. & Dickinson, M., 2014, Cosmic Star-Formation History, ARA&A,52,415

Siebenmorgen, R. & Krügel, E., 2007, Dust in starburst nuclei and ULIRGs. SED models for observers, A&A, 461, 445

Rujopakarn W., Rieke, G. H., Weiner, B. J., 2013, Mid-Infrared Determination of Total Infrared Luminosity and Star Formation Rates of Local and High-Redshift Galaxies, ApJ, 767, 73